

Short Communication

# One-step Nanocasting Synthesis of Mesostructured TiO<sub>2</sub>/graphitic Carbon Composite as an Anode Material for Lithium-Ion Battery

Bo Li<sup>1</sup>, Qianyu Zhang<sup>1</sup>, Chengli Zhang<sup>1</sup>, Shifei Kang<sup>1</sup>, Xi Li<sup>1,\*</sup>, Yangang Wang<sup>2,\*</sup>

<sup>1</sup>Department of Environmental Science and Engineering, Fudan University, Shanghai 200433, China

<sup>2</sup>Department of Environmental Science and Engineering, University of Shanghai for Science and Technology, Shanghai 200093, China

\*E-mail: [xi\\_li@fudan.edu.cn](mailto:xi_li@fudan.edu.cn); [ygwang8136@gmail.com](mailto:ygwang8136@gmail.com)

Received: 14 April 2013 / Accepted: 16 May 2013 / Published: 1 June 2013

---

Mesostructured TiO<sub>2</sub>/graphitic carbon (TiO<sub>2</sub>-GC) composite was synthesized by a simple one-step nanocasting method. The as-prepared material was characterized by X-ray diffraction, transmission electron microscopy and Brunauer–Emmer–Teller. The results show that the mesostructured TiO<sub>2</sub>-GC composite has a moderate specific surface area (263.05 m<sup>2</sup> g<sup>-1</sup>) and large pore volume (0.211 m<sup>3</sup> g<sup>-1</sup>), which are beneficial for Li<sup>+</sup> ion diffusion during charge-discharge processes. The electrochemical tests exhibit that the TiO<sub>2</sub>-GC composite possesses a high initial discharge capacity of 1076 mAh g<sup>-1</sup>, and the discharge capacity still remains 326 mAh g<sup>-1</sup> at 50th cycle. Therefore, TiO<sub>2</sub>-GC composite may be considered as a promising anode material for lithium-ion battery due to its excellent reversibility and cyclability.

---

**Keywords:** One-step nanocasting; Mesostructured; TiO<sub>2</sub>/graphitic carbon; lithium-ion battery

## 1. INTRODUCTION

Rechargeable lithium-ion battery is currently utilized for portable electronic devices and considered as a promising power source in electric vehicles and hybrid electric vehicles [1-4]. It is expected to have superior performance in terms of energy density, cycling life, and high-rate capability for the new generation lithium-ion battery, which should be developed by achieving breakthroughs in electrode materials [5]. As a potential anode material, titanium oxide (TiO<sub>2</sub>) has received considerable interest as an alternative material to the current graphite electrode (theoretical capacity 372 mAh g<sup>-1</sup>) due to its superior safety, low volume change (< 4% for Li<sub>x</sub>TiO<sub>2</sub>, 0 ≤ x ≤ 1), environmental

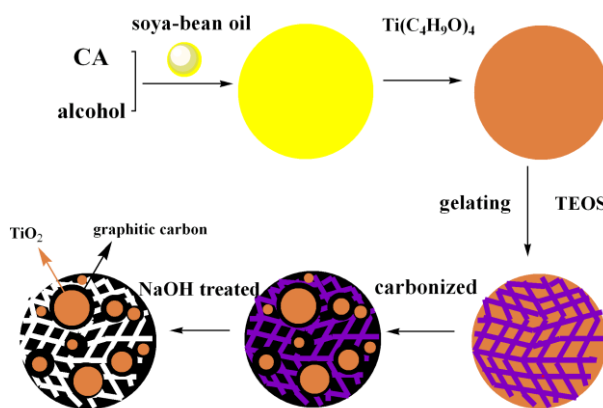
friendliness, low cost, and high chemical stability [6-8]. However, the application of TiO<sub>2</sub> to lithium-ion batteries is generally limited by the low electronic conductivity of TiO<sub>2</sub> ( $\sim 10^{-12}$  to  $10^{-7}$  S cm<sup>-1</sup>) and Li-ion diffusivity ( $\sim 10^{-15}$  to  $10^{-9}$  S cm<sup>2</sup> S<sup>-1</sup>), which severely cause rapid capacity fading [9-11]. In order to overcome these disadvantages, several methods including titanium-based nanostructures [12-15], anatase TiO<sub>2</sub> thin films [16] and TiO<sub>2</sub>-based carbon composites [7-9] have been investigated. In these cases, TiO<sub>2</sub>-based carbon composites have attracted special attention since carbon materials can provide good electrical contact [17-19]. However, up to date, the fabrication of TiO<sub>2</sub>/C composite was either too expensive or inconvenient to be viable for large-scale applications. Therefore, a simple and effective method to synthesize the mesostructured TiO<sub>2</sub>/carbon composite remains essential and challenging. Moreover, the framework of the obtained carbon materials in the composites is an amorphous structure which leads to a relatively low electrical conductivity and prevents the rapid Li<sup>+</sup> insertion/extraction during the discharge-charge process [20].

Graphitic carbon, due to its high surface area, high electronic conductivity and unique mechanical properties, has been considered as a functional material to improve electronic conductivity for lithium-ion battery [21, 22]. In this paper, we report a simple method for the synthesis of mesostructured TiO<sub>2</sub>/graphitic carbon composite by one-step nanocasting route. One of the most prominent advantages of this method is its facile operation and enlargement, and the formed mesostructured TiO<sub>2</sub>/graphitic carbon composite possesses a moderate specific surface area and large pore volume. The results showed that this TiO<sub>2</sub>/GC composite exhibited excellent cyclability and low the charge transfer resistance, giving their potential applications as anode materials for lithium-ion battery.

## 2. EXPERIMENTAL

### 2.1 Preparation of mesostructured TiO<sub>2</sub>/graphitic carbon composite

Mesostructured TiO<sub>2</sub>/graphitic carbon composite was prepared by one-step nanocasting route and the synthesis strategy was illustrated in Scheme.1. The synthesis was achieved using tetrabutyl titanate and soybean oil as Ti source and carbon precursor, respectively, for the gelation reaction of tetraethyl orthosilicate and citric acid. In a typical synthesis, 8.4 g (40 mmol) of citric acid and 8.4 g of soybean oil were dissolved in 80 ml of alcohol, then 6.81 g (20 mmol) tetrabutyl titanate (Ti(C<sub>4</sub>H<sub>9</sub>O)<sub>4</sub>) was added to the above solution under magnetic stirring to until complete homogenization. Subsequently, 8.3 g (40 mmol) tetraethyl orthosilicate (TEOS) was dropped into the above solution under vigorous stirring, after stirring for 2 h, the mixture was transferred to petri plate and kept still at the room temperature for 24 h. After that, this as-prepared sample was carbonized at 900 °C for 4 h under Ar flow with a heating rate of 2 °C min<sup>-1</sup>, the resulting composite was treated with 2M NaOH aqueous solution for several times to remove the silica and the TiO<sub>2</sub>/GC composite with a graphitic carbon framework was obtained. Graphitic carbon (GC) was prepared by the same method but without adding tetrabutyl titanate in the above experimental process.



**Scheme 1.** Illustration for the synthesis of mesostructured  $\text{TiO}_2$ /graphitic carbon composite by one-step nanocasting route.

## 2.2 Structural characterization

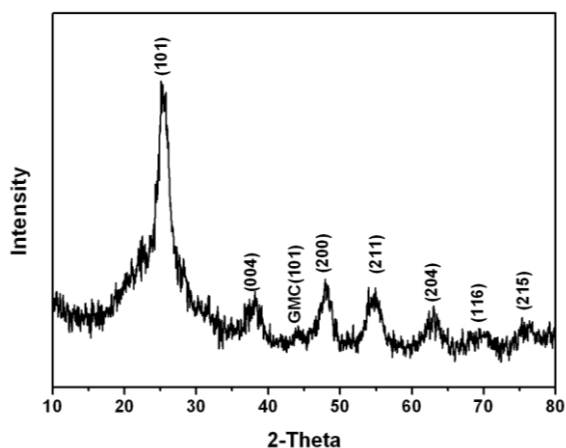
X-ray diffraction (XRD) patterns were collected in  $\theta$ - $2\theta$  mode using Rigaku D/MAX-2550VB/PC diffractometer ( $\text{CuK}\alpha 1$  radiation,  $\lambda = 1.5406 \text{ \AA}$ ), operated at 40 kV and 100 mA. The microstructure of the as-prepared samples was investigated by a transmission electron microscope (TEM), which were taken using a JEOL JEM-2010 electron microscope with an acceleration voltage of 200 KV. Nitrogen sorption isotherms were performed at  $-196 \text{ }^\circ\text{C}$  on a Micromeritics ASAP 2000 apparatuses. The specific surface area of the as-prepared materials was calculated by Brumauer–Emmett–Teller (BET) method. The pore volume and pore size distributions were obtained from the desorption branches of the isotherms using the Barrett–Joyner–Halanda (BJH) method.

## 2.3 Electrochemical measurements

Electrochemical measurements were performed using home-made coin cells with lithium metal as the counter and reference electrodes at room temperature. The working electrodes were prepared by coating the slurry of the active materials (85 wt%), carbon black (10 wt%), and polyvinylidene fluoride (PVDF) (5 wt%) dissolved in *n*-methyl-2-pyrrolidone onto a Cu foil substrate. The coated electrodes were dried in a vacuum oven at  $120 \text{ }^\circ\text{C}$  for 10 h to evaporate the NMP solvent. The electrolyte was 1M  $\text{LiPF}_6$  in a mixture of ethylene carbonate, diethyl carbonate and ethylmethyl carbonate (1:1:1 by volume), and Celgard 2400 was used as the separator. Cell assembly was carried out in an argon-filled glove-box (with the concentrations of moisture and oxygen below 1ppm). The electrochemical performance was tested at 0.2 C on Land CT2001A (Wuhan, China). Electrochemical impedance spectra (EIS) measurements were measured at the electrochemical workstation (CHI 660E) with a  $\pm 5 \text{ mV}$  AC signal and a frequency range from 10 MHz to 1 MHz. All experiments were carried out at room temperature ( $25 \text{ }^\circ\text{C}$ ).

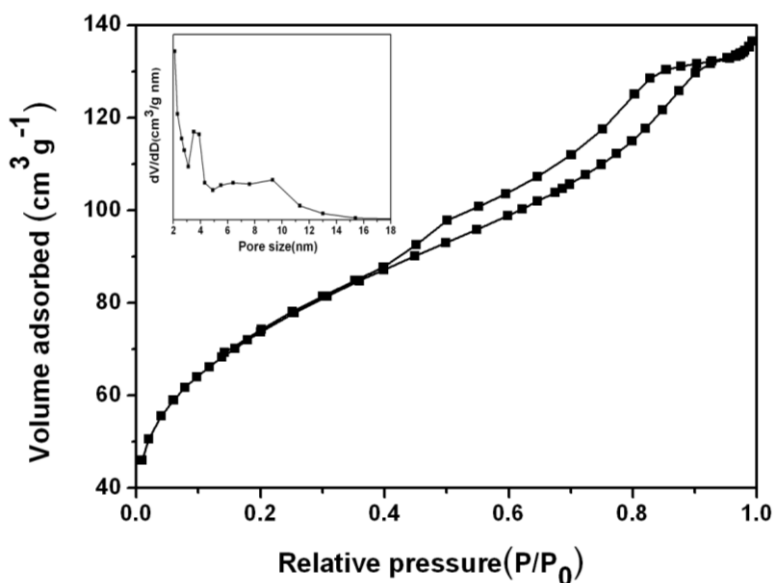
### 3. RESULTS AND DISCUSSION

#### 3.1 Characteristics of TiO<sub>2</sub>/GC



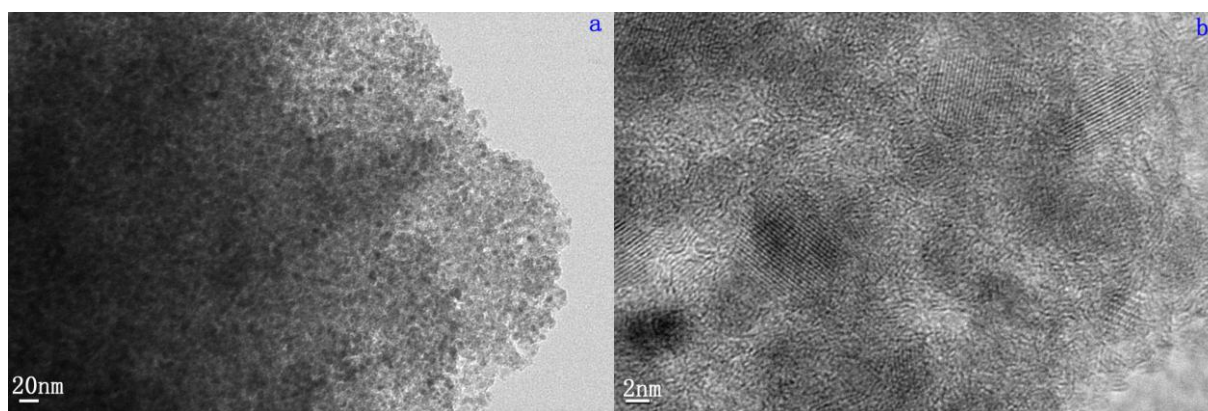
**Figure 1.** XRD patterns of the TiO<sub>2</sub>/GC composite.

Fig.1 presents X-ray diffraction patterns (XRD) of mesostructured TiO<sub>2</sub>/GC composite. It can be seen that the diffraction pattern located at about  $2\theta = 25, 38, 48, 55, 63, 68$  and  $75^\circ$  can be indexed to (101), (004), (200), (211), (204), (116) and (215) crystal planes of anatase TiO<sub>2</sub>, which are in accordance with the standard values (JCPDS no. 21-1272). In addition, it can be observed that a broad peak appeared near  $2\theta = 44^\circ$  can be assigned as the (101) reflection of the graphitic carbon. Besides, the peak appeared around  $2\theta = 25^\circ$  corresponding to (002) orientations of graphitic carbon unable to distinguish, which could be ascribed to overlapping with TiO<sub>2</sub> (101) peak.



**Figure 2.** Nitrogen adsorption-desorption isotherms and pore size distribution curves (inset) of the TiO<sub>2</sub>/GC composite.

Fig.2 gives the nitrogen adsorption-desorption isotherms and corresponding Barrette-Joynere-Halenda (BJH) pore size distribution curves for the mesostructured  $\text{TiO}_2/\text{GC}$  composite. The isotherm exhibits a representative Langmuir IV curve with a clear  $\text{H}_1$ -type hysteresis loop at a relative pressure of 0.4-1.0, which implies the existence of mesoporosity. The pore size distribution obtained from an analysis of desorption branch of the isotherms is shown in the inset of Fig. 2, it can be seen that this composite has uniform pore size distributions centered at about 3.2 nm, which can be ascribed to the dissolution of the silica template. Besides, the  $\text{TiO}_2/\text{GC}$  composite has a moderate BET surface area of  $263.05 \text{ m}^2 \text{ g}^{-1}$ , and a large pore volume of  $0.211 \text{ m}^3 \text{ g}^{-1}$ , which are beneficial for lithium ion battery with a high specific capacity during discharge-charge process [20].



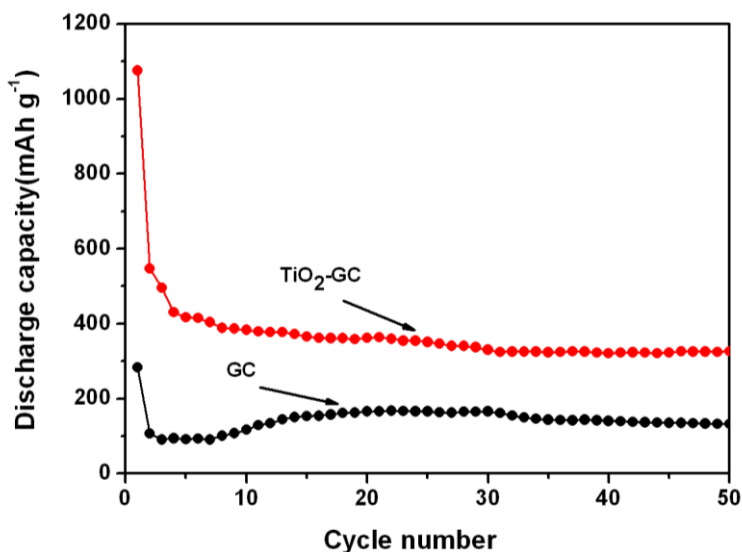
**Figure 3.** (a) TEM image and (b) HRTEM image of mesostructured  $\text{TiO}_2/\text{graphitic carbon}$  composite.

Fig.3 shows transmission electron microscopy (TEM) images of the mesostructured  $\text{TiO}_2/\text{GC}$  composite. It can be seen that there are no evident big particles that related to  $\text{TiO}_2$  particle can be detected from low-magnification TEM images, indicating  $\text{TiO}_2$  with ultrafine nanocrystals is uniformly dispersed into the mesostructured carbon matrix, which is consistent with the XRD investigation. The further high-magnification TEM (HRTEM) images (Fig.3b) confirmed  $\text{TiO}_2$  particles are covered by the walls of graphitic carbon which can function as efficient electron transport pathways and improve electrical conductivity.

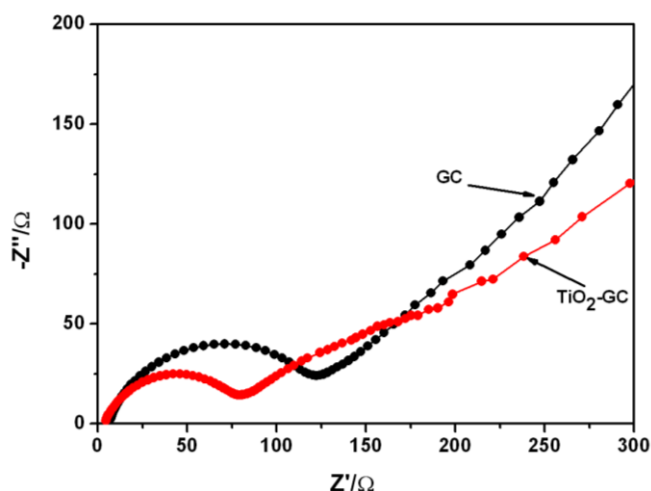
### 3.2 Electrochemical performance

Fig.4 compares the cycling performance of the  $\text{TiO}_2\text{-GC}$  composite and GC electrodes. The initial discharge capacities of  $\text{TiO}_2\text{-GC}$  and GC electrodes are  $1076$  and  $283 \text{ mAh g}^{-1}$  at a rate of  $0.2 \text{ C}$ , respectively. It can be seen that GC electrode undergoes slight capacity increasing in the range of 10 to 30 cycles, but the capacity gradually decreased to  $133 \text{ mAh g}^{-1}$  after 50 cycles. In addition, although there was a drop in the capacity of  $\text{TiO}_2\text{-GC}$  in the first few cycles, the discharge capacity still remains at  $326 \text{ mAh g}^{-1}$  after 50 cycles, much more than twice of the value for graphite carbon. Moreover, the

TiO<sub>2</sub>-GC composite exhibits high electrode coulombic efficiency approaching 98.7% from 30 to 50 cycles.



**Figure 4.** Comparison of the cycle performances of the TiO<sub>2</sub>-GC composite and graphitic carbon at a current rate of 0.2 C



**Figure 5.** the electrochemical impedance spectra (EIS) of TiO<sub>2</sub>-GC composite and graphitic carbon

Fig.5 shows the EIS of TiO<sub>2</sub>-GC composite and graphitic carbon. The EIS indicate that each curve is composed of a depressed semicircle in the high and intermediate frequency ranges and a straight line in the low frequency region. The high frequency semicircle is related to the charge transfer resistance at the active material interface, while the sloping line at the low frequency end indicates the Warburg impedance caused by a semi-infinite diffusion of Li<sup>+</sup> ion in the electrode [23]. As seen from Fig.5, the charge transfer resistance of TiO<sub>2</sub>-GC is much smaller than that of the GC, which could be ascribed to the presence of TiO<sub>2</sub> in the composite that can restrain the formation of surface film [24].

#### 4. CONCLUSION

In conclusion, we have demonstrated a simple one-step nanocasting route for the synthesis of mesostructured TiO<sub>2</sub>/GC composite. XRD and TEM results show that the formed anatase TiO<sub>2</sub> particles are well dispersed in the graphitic carbon matrix. Nitrogen sorption reveal this TiO<sub>2</sub>/GC composites possess uniform mesostructure, moderate BET surface area, and large volume. The electrochemical tests show TiO<sub>2</sub>/GC composite exhibited more excellent cyclability and lower the charge transfer resistance than GC, which could be ascribed to the combined functionalities of TiO<sub>2</sub> and graphitic carbon, TiO<sub>2</sub> can restrain the formation of surface film and graphitic carbon can improve electronic conductivity of the composite. Therefore, TiO<sub>2</sub>-GC composite may be considered to be a promising anode material for lithium-ion battery in future.

#### ACKNOWLEDGMENTS

This work was carried out with financial supports from National Natural Science Foundation of China (No. 61171008, 21103024), China Postdoctoral Science Foundation Special Funded Project (Grant No.201104236), and the funds from Dalian Mingjia Jinshu Products Limited Company, Suzhou Baotan New Energy Limited Company and Shanghai Jubo Energy Technology Limited Company (China).

#### References

1. J.M. Tarascon and M. Armand, *Nature*, 414 (2001) 359.
2. Y. Idota, T. Kubota, A. Matsufuji, Y. Maekawa, T. Miyasaka, *Science*, 276 (1997) 1395.
3. Q.Y. Zhang and X. Li, *Int. J. Electrochem. Sci.*, 8 (2013).
4. Q.Y. Zhang, *Int. J. Electrochem. Sci.*, 8 (2013).
5. Y.G. Liu, H.Y. Wang, B. Jin, Z.Z. Yang, W. Qi, Y.C. Liu and Q.C. Jiang, *Int. J. Electrochem. Sci.*, 8 (2013) 4797
6. S.G. Lee, H.G. Deng, J. Hu, L.H. Zhou and H. L. Liu, *Int. J. Electrochem. Sci.*, 8 (2013) 2204.
7. P.Y. Chang, C.H. Huang and R. Doong, *Carbon*, 50 (2012) 4259.
8. K.Y. Kang, Y.G. Lee, S. Kim, S.R. Seo, J.C. Kim and K.M. Kim, *Mater. Chem. Phys.*, 137 (2012) 169.
9. S.J. Park, H. Kim, Y.J. Kim and H. Lee, *Electrochim. Acta*, 56 (2011) 5355.
10. S.J. Park, Y.J. Kim and H. Lee, *J. Power Sources*, 196 (2011) 5133.
11. L.J. Fu, H. Liu, H.P. Zhang, C. Li, T. Zhang, Y.P. Wu and H.Q. Wu. *J. Power Sources*, 159 (2006) 219.
12. Q.J. Li, J.W. Zhang, B.B. Liu, M. Li, R. Liu, X.L. Li, H.L. Ma, S.D. Yu, L. Wang, Y.G. Zou, Z.P. Li, B. Zou, T. Cui and G.T. Zou, *Inorg. Chem.*, 47 (2008) 9870.
13. H. Zhang, G.R. Li, L.P. An, T.Y. Yan, X.P. Gao and H.Y. Zhu, *J. Phys. Chem.*, 111 (2007) 6143.
14. X.P. Gao and H.X. Yang, *Energy Environ. Sci.*, 3 (2010) 174.
15. D.W. Liu and G.Z. Cao, *Energy Environ. Sci.*, 3 (2010) 1218.
16. M.J. Lindsay, M.G. Blackford, D.J. Attard, V. Luca, M. Skyllas-Kazacos and C.S. Griffith, *Electrochim. Acta*, 52 (2007) 6401.
17. Y. Yu, L. Gu, C.B. Zhu, P.A. Van Aken and J. Maier, *J. Am. Chem. Soc.*, 131 (2009) 15984.
18. J.Z. Chen, L. Yang, S.H. Fang and S.Hirano, *Electrochem. Commun.*, 13 (2011) 848.
19. J. Hassoun, K.S. Lee, Y.K. Sun and B. Scrosati, *J. Am. Chem. Soc.*, 133 (2011) 3139.
20. Y.G. Wang, B. Li, C.L. Zhang, T. Hong, S.F. Kang, S. Jiang and X. Li, *J. Power Sources*, 219

(2012) 89.

21. B. Lee, Y. Chen, F. Duerr, D. Mastrogiovanni, E. Garfunkel, E.Y. Andrei and V. Podzorov, *Phys. Status Solidi (B)*, 244 (2007) 4106.
22. Y.H. Ding, P. Zhang, H.M. Ren, Q. Zhuo, Z.M. Yang and Y. Jiang, *Mater. Res. Bull.*, 46 (2011) 2403.
23. Q.Y. Zhang, C.L. Zhang, B. Li, S.F. Kang, X. Li and Y.G. Wang, *Electrochim. Acta*, 98 (2013) 146.
24. H. Huang, W.K. Zhang, X.P. Gan, C. Wang and L. Zhang, *Mater. Lett.*, 61 (2007) 296.